# Response Surface Approach to Optical Channel Dropping Filter Design Parameters Optimization

H.Hazura, F.Aliman, A.S.M. Zain, A.R Hanim, F.Salehuddin, S.K Idris and M.Z Nor Syaimaa
*Centre for Telecommunications Research Innovations (CETRI),*
*Faculty of Electronic & Computer Engineering, Universiti Teknikal Malaysia Melaka,*
*76100 Durian Tunggal, Melaka.*
*hazura@utem.edu.my*

***Abstract*—The objective of this paper is to optimise the design parameters for the optical channel dropping filter, which is based on the microring resonator topology. The most important parameters to determine the performance of the microring channel optical filter are the waveguide width, gap, core thickness and ring radius. The determination of parameters by classical experimental design methods requires a large amount of experimental data, which has been found to be costly and time-consuming. To overcome this drawback, a design of experiment (DOE) methods of the Response Surface Methodology (RSM) was employed. This paper employed the RSM design analysis in evaluating the performance of the microring resonator with different design parameters settings. Upon completion, the RSM shows that the optimum condition can be achieved when the ring radius is 5.50µm, a gap of 200nm, waveguide width of 418 nm and core thickness of 220 nm. In conclusion, for optimized performance of the channel dropping filter, design conditions within the range demonstrated in this study are suggested.**

***Index Terms*—Response Surface Methodology; Optical Channel Dropping Filter; Microring Resonator**

## I. INTRODUCTION

Silicon-on-insulator (SOI) has emerged to be an attractive technology, which plays a significant role in the realisation of miniaturisation of photonic integrated circuits. The beauty of SOI configuration lies on the high-index-contrast between the core (silicon) and the bottom cladding material (silicon dioxide). This configuration permits the sub-wavelength light confinement in the core with minimal optical leakage into the silicon substrate [1-3]. By having this feature, SOI has become the most suitable option for the production of the microring channel dropping filter, which is well known as a highly integrated photonic device with very sharp bends. Microring resonators are versatile wavelength-selective elements that can be used to create a wide class of optical filter [4-7].

Selecting the most appropriate parameter is the primary challenge in designing and fabricating the SOI microring channel dropping filter. The performance of the microring channel dropping filter is influenced by several parameters including the waveguide width, gap, core thickness and ring radius. The design of experimental (DOE) methods, such as the Taguchi method, factorial design and the Response Surface Methodology (RSM) are widely used in order to optimise the design parameters [9-10]. These analytical tools are outstanding in determining the design parameter variation effect. In this paper, the RSM method was adopted to identify the most significant design parameter and optimise the Q-factor value of the optical channel dropping filter.

## II. OPTICAL CHANNEL DROPPING FILTER MATHEMATICAL MODELLING

Figure 1 illustrates the principle behind the operation of the optical channel dropping filter based on the microring resonator topology. The resonances occur when the optical path length of a round-trip is multiple of the effective wavelength. If the microring is on resonant, the light will be coupled into the ring waveguide and exited at the drop port. Otherwise, the light will be transferred to the through port [11-12].

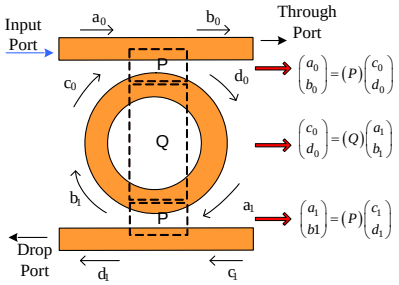


Figure 1: Schematic diagram of channel dropping filter

For the transmission of the input and output waveguide, $P$ can be calculated by [13]:

$$P = \frac{1}{\kappa}\begin{pmatrix} -t & 1 \\ -1 & t^{*} \end{pmatrix} \tag{1}$$

where $\kappa$ is the coupling coefficient, and $\kappa^2$ determines the ratio of the power coupled between the bus and ring waveguides. By assuming the case of lossless coupling, we have $\kappa^2+t^2=1$, where $t$ is the transmission coefficient.

As the light propagates around the ring, it accumulates a phase shift and attenuated. The optical phase delays and the waveguide loss, Q can be described as:

$$Q = \frac{1}{\kappa}\begin{pmatrix} 0 & e^{-i\tilde{\beta}\pi R} \\ e^{i\tilde{\beta}\pi R} & 0 \end{pmatrix} \tag{2}$$

where $R$ is the ring radius and $\beta$ is the propagation constant, which is equal to:

$$\tilde{\beta} = \frac{2\pi}{\lambda_o} n_{eff} - j\frac{\alpha}{2} \quad (3)$$

Here, $\alpha$ is the loss per unit length in the microring, $\lambda_o$ is the free space wavelength and $n_{eff}$ is the effective refractive index. The transfer matrix between the two straight waveguides is:

$$\begin{pmatrix} a_0 \\ b_0 \end{pmatrix} = (PQP)\begin{pmatrix} c_1 \\ d_1 \end{pmatrix} \equiv (M)\begin{pmatrix} c_1 \\ d_1 \end{pmatrix} \equiv \begin{pmatrix} m_{11} & m_{12} \\ m_{21} & m_{22} \end{pmatrix}\begin{pmatrix} c_1 \\ d_1 \end{pmatrix} \quad (4)$$

Considering only one input, $c_1$ will be zero, hence, the final transfer functions for the drop port |D| signals, where the Q-factor value is observed is:

$$|D| = \frac{d_1}{a_0} = \frac{1}{m_{12}} = \frac{-\sqrt{\kappa_{in}\kappa_{out}}\, e^{-i\tilde{\beta}\pi R}}{1-\sqrt{(1-\kappa_{in})(1-\kappa_{out})}\, e^{-i\tilde{\beta}2\pi R}} \quad (5)$$

In general, Q-factor can be used to predict the resonator's ability to circulate and store the input signal. The Q-factor is determined by the following equation [14]:

$$Q \approx \frac{\lambda_R}{\Delta\lambda_{3dB}} \quad (6)$$

where $\lambda_R$ is the resonant wavelength, and $\lambda_{3dB}$ is the 3db wavelength.

## III. Methodology

The performance of the channel dropping optical filter regarding Q-factor was investigated by optimising four design parameters, such as ring radius (A), gap separation between the ring waveguide and bus waveguide (B), Waveguide width (C), core thickness (D). Figure 2 (a) and (b) portray a layout and the cross-section view of the channel dropping filter.

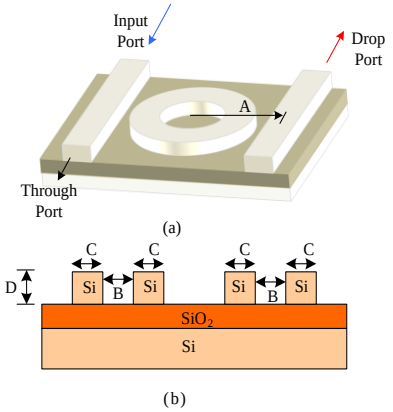


Figure 2: (a) Layout and (b) cross-section of the channel dropping filter.

A standard RSM design called the D–optimal design was used to determine the main and interaction effects of all the process parameters. The RSM-CCD analysis was carried out by using the State-Ease Design Expert software, which had a desirability function for the multi-response optimisation in order to determine the main and interaction effect of all parameters [15-17]. Table 1 shows a list of design parameters where their levels were varied according to the RSM-CCD experimental setup. It indicates the low (-) and high (+) levels and the ranges of all the factors studied.

Table 1
Experimental Setup for Design Parameters Using RSM-CCD

| Symbol | Control Factors | Units | (-) level | (+) level |
|---|---|---|---|---|
| A | Ring Radius | μm | 5.5 | 6.5 |
| B | Gap | nm | 100 | 200 |
| C | Waveguide Width | nm | 400 | 420 |
| D | Core Thickness | nm | 120 | 220 |

The observed data from the experimental runs are then fed into the Design Expert to optimise and establish a predictive mathematical model to estimate the Q-factor. This analysis was carried out for a level of confidence not less than 95 %, which is the criterion to be set into the RSM. Predicted values of the responses for these optimised values were computed by using the quadratic equation defined, which considers only significant parameters.

## IV. Results and Discussion

The influence of ring radius, gap, waveguide width and core thickness was investigated through the modelling stages. Twenty-nine experiments for optimising the Q-factor value were conducted. The experimental conditions and Q-factor value (Q) for each case are presented in Table 2.

Table 2
Experimental Design and Response

| No. | Ring Radius | Gap | Waveguide Width | Core Thickness | Q |
|---|---|---|---|---|---|
| 1 | 5.80 | 200.00 | 419.99 | 219.95 | 9192.79 |
| 2 | 5.77 | 199.85 | 420.00 | 220.00 | 9253.53 |
| 3 | 5.92 | 200.00 | 420.00 | 219.99 | 8993.62 |
| 4 | 5.99 | 199.97 | 420.00 | 220.00 | 8854.98 |
| 5 | 5.52 | 200.00 | 419.76 | 220.00 | 9697.19 |
| 6 | 5.51 | 199.69 | 420.00 | 220.00 | 9700.77 |
| 7 | 6.08 | 200.00 | 420.00 | 220.00 | 8689.84 |
| 8 | 5.78 | 198.74 | 420.00 | 220.00 | 9170.90 |
| 9 | 5.97 | 200.00 | 420.00 | 219.02 | 8855.25 |
| 10 | 5.99 | 199.28 | 420.00 | 220.00 | 8817.54 |
| 11 | 6.26 | 200.00 | 420.00 | 220.00 | 8381.68 |
| 12 | 6.04 | 198.33 | 420.00 | 219.99 | 8681.51 |
| 13 | 6.27 | 200.00 | 420.00 | 220.00 | 8360.61 |
| 14 | 5.50 | 199.99 | 418.37 | 220.00 | 9706.89 |
| 15 | 6.32 | 200.00 | 420.00 | 220.00 | 8275.11 |
| 16 | 6.33 | 199.25 | 420.00 | 220.00 | 8213.65 |
| 17 | 6.41 | 199.98 | 420.00 | 220.00 | 8108.01 |
| 18 | 6.36 | 199.35 | 420.00 | 220.00 | 8167.57 |
| 19 | 6.36 | 198.51 | 420.00 | 220.00 | 8106.25 |
| 20 | 6.01 | 200.00 | 413.93 | 220.00 | 8699.79 |
| 21 | 6.44 | 199.94 | 417.20 | 220.00 | 7996.45 |
| 22 | 6.50 | 200.00 | 417.55 | 220.00 | 7893.72 |
| 23 | 6.46 | 200.00 | 416.18 | 220.00 | 7931.70 |
| 24 | 6.50 | 200.00 | 408.46 | 219.89 | 7702.87 |
| 25 | 5.50 | 177.57 | 420.00 | 220.00 | 8505.23 |
| 26 | 5.71 | 199.51 | 400.00 | 220.00 | 8931.96 |
| 27 | 6.50 | 200.00 | 403.81 | 219.52 | 7590.64 |
| 28 | 5.50 | 174.94 | 417.86 | 220.00 | 8325.26 |
| 29 | 6.50 | 200.00 | 402.11 | 219.62 | 7560.36 |

The models for the performance of the optical channel dropping filter were developed to evaluate the relationship of the design parameters with the Q-factor value. The statistical significance of the model was evaluated by the values of F, and P, as presented in Table 3.

Table 3
Analysis of variance (ANOVA) for Q-factor

| Source | Sum of Squares | df | Mean Square | F-value | P-value |
|---|---|---|---|---|---|
| Model | 1.846E+008 | 4 | 4.615E+007 | 23.13 | < 0.0001 |
| A | 1.102E+007 | 1 | 1.102E+007 | 5.53 | 0.0319 |
| B | 1.023E+008 | 1 | 1.023E+008 | 51.28 | < 0.0001 |
| C | 5.731E+005 | 1 | 5.731E+005 | 0.29 | 0.5993 |
| D | 7.071E+007 | 1 | 7.071E+007 | 35.44 | < 0.0001 |
| Residual | 3.192E+007 | 16 | 1.995E+006 | | |
| Lack of Fit | 3.192E+007 | 12 | 2.660E+006 | | |
| Pure Error | 0.000 | 4 | 0.000 | | |
| Cor Total | 2.165E+008 | 20 | | | |

In Table 3, the significance of the model is revealed according to the F-value of 23.13 model. There was only a probability of 0.01% of the noise in this "F-Value model". If the values of "Probability>F", and if they are lesser than 5% (0.05), then the model is said to be sound; thus, A, B and D are considered an excellent model terms. In case the values are higher than 0.1 (10%), the model terms are said to be insignificant and impractical to be considered.

The three dimensional (3D) surface plots for the Q-factor concerning the significant control parameters are depicted in Figure 3. Two significant control parameters were varied while the other process parameters were fixed at the middle value in both of the plots. The gap and ring radius are two parameters affecting the Q-factor. According to Figure 3(a), a bigger gap at a smaller ring radius gives a high Q-factor. On the other hand, Figure 3(b) reveals that Q-factor is proportional to the gap size regardless of the value of waveguide width. The insignificance of the waveguide width control factor is understandable as the P-value shown in Table 3 is more than 0.05 for this parameter as has been identified in the earlier stage of the analysis. It should be noted that the effect of increasing the core thickness will increase the Q-factor, which is clearly visible in Figure 3(c). The 3D surface in this figure also confirms the insignificance of waveguide width parameter. In Figure 3(d), smaller ring radius with higher core thickness produces a higher Q-factor. From the three-dimensional surface plots of the Q-factor, we may observe that the ring radius is inversely proportional to the Q-factor while the gap and core thickness is directly proportional to the Q-factor. High Q-factor can be obtained by increasing the gap and core thickness. The waveguide width is insignificant and does not influence either in increasing or decreasing the Q-factor.

This result is in agreement with a study of the Design Modelling and Characterizations of SOI-based Parallel Cascaded MRR Array (PCMRRA) by the Coupled Mode Theory [12]. The study concluded that as the gap increases, the Q-factor and insertion loss raised. Therefore, an accurate selection of gap separation value is crucial to confirm a well-functioning device. The study also concluded that the Q-factor is highly dependent on the ring radius.

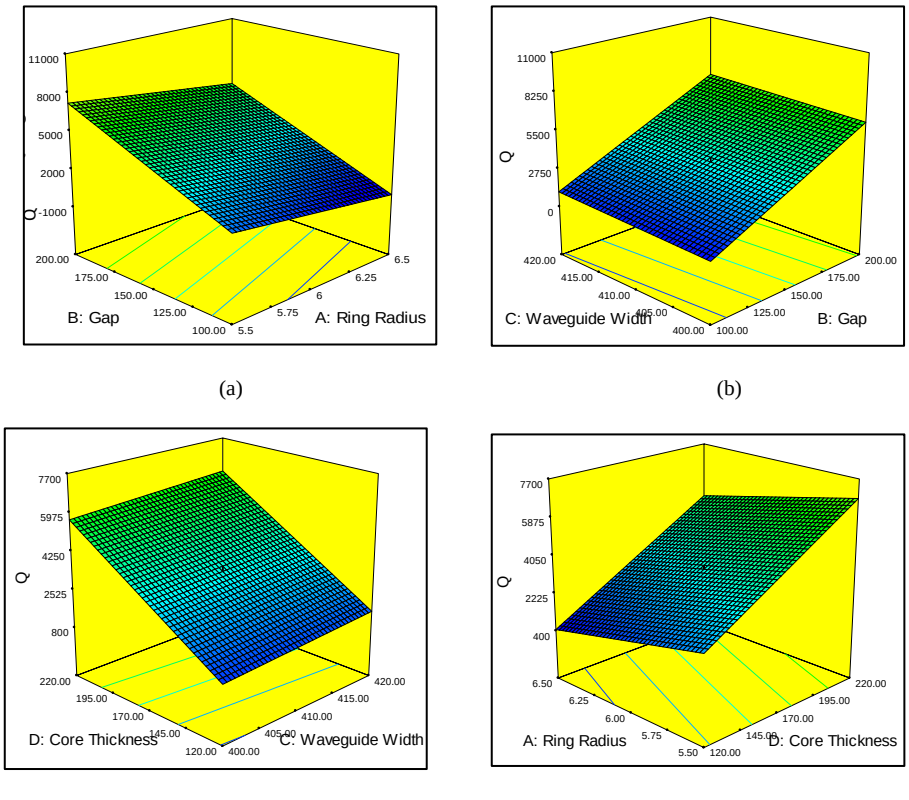


(a) (b) (c) (d)

Figure 3: 3D surface of Q-factor model; (a) effects of gap and ring radius, (b) effects of waveguide width and gap, (c) effects of core thickness and waveguide width, (d) effects of ring radius and core thickness

### *A. Mathematical Modelling*

The predictive model was developed to evaluate the relationship of the device parameters variations to the Q-factor. Through this model, the experimental results of the Q-factor by any combination of device parameters variations can be estimated. The model can be used to re-create the

results of this experiment. However, it could not be used for modelling future responses. The Q-factor was modelled and expressed as a function of the ring radius, gap, waveguide width and core thickness. Equation (7) shows the final equation regarding the actual code for the Q-factor [18].

$$\mathbf{Q} = +3625.43 - 898.41*A + 2736.72*B + 204.84*C + 2275.37*D \quad (7)$$

### B. Optimization using Desirability Criterion

The ranges and goals of the process parameters are the ring radius, gap, waveguide width and waveguide height as well as the device characteristics, which in this study is the Q-factor as provided in Table 4. The Q-factor was assigned to an importance of 4. Meanwhile, all the process parameters were assigned to an importance of 3. "Importance" is a tool for changing the relative priorities to achieve goals established for some or all variables. If the study would like to emphasise one over the rest, the importance is set higher. Design-Expert offers five levels of importance ranging from 1 plus (+) to 5 plus (+++++). For this study, the Importance field is left at 3 plus (+++), a medium setting. By leaving all importance criteria at their defaults, no goals are favoured over the rest.

Table 4
Range of Process Parameters and Response for Desirability

| Name | Ring Radius | Gap | Waveguide Width | Core Thickness | Q |
|---|---|---|---|---|---|
| Goal | is in range | is in range | is in range | is in range | maximize |
| Lower Limit | 5.5 | 100 | 400 | 120 | 534 |
| Upper Limit | 6.5 | 200 | 420 | 220 | 11236 |
| Lower Weight | 1 | 1 | 1 | 1 | 1 |
| Upper Weight | 1 | 1 | 1 | 1 | 1 |
| Importance | 3 | 3 | 3 | 3 | 4 |

Table 5 shows the optimal set of a solution with a higher desirability function that is required for obtaining the desired device characteristics under a specified constraint. The optimum condition is when the Q-factor of 9706.89 can be achieved when the ring radius is 5.50 µm, a gap of 199.99 nm, waveguide width of 418.37 nm and core thickness of 220 nm (experiment 14).

### C. Confirmation test

The results obtained after the optimisation was verified by conducting the experiments under the optimised conditions of all the factors. The confirmation test was conducted to verify the results using the optimised predicted control factors valued from the RSM using Design Expert and the actual values from mathematical modelling that were developed using MATLAB as described in section II. Figure 4 depicts the drop port response by mathematical modelling where the optimised design parameters from the RSM were employed. From the output channel response, the Q-factor was calculated using Equation (6).

Table 5
Optimization Using Desirability Criterion

| No. | Ring Radius | Gap | Waveguide Width | Core Thickness | Q | Desirability |
|---|---|---|---|---|---|---|
| 1 | 5.80 | 200.00 | 419.99 | 219.95 | 9192.79 | 0.75 |
| 2 | 5.77 | 199.85 | 420.00 | 220.00 | 9253.53 | 0.75 |
| 3 | 5.92 | 200.00 | 420.00 | 219.99 | 8993.62 | 0.75 |
| 4 | 5.99 | 199.97 | 420.00 | 220.00 | 8854.98 | 0.75 |
| 5 | 5.52 | 200.00 | 419.76 | 220.00 | 9697.19 | 0.75 |
| 6 | 5.51 | 199.69 | 420.00 | 220.00 | 9700.77 | 0.75 |
| 7 | 6.08 | 200.00 | 420.00 | 220.00 | 8689.84 | 0.75 |
| 8 | 5.78 | 198.74 | 420.00 | 220.00 | 9170.90 | 0.75 |
| 9 | 5.97 | 200.00 | 420.00 | 219.02 | 8855.25 | 0.75 |
| 10 | 5.99 | 199.28 | 420.00 | 220.00 | 8817.54 | 0.75 |
| 11 | 6.26 | 200.00 | 420.00 | 220.00 | 8381.68 | 0.75 |
| 12 | 6.04 | 198.33 | 420.00 | 219.99 | 8681.51 | 0.75 |
| 13 | 6.27 | 200.00 | 420.00 | 220.00 | 8360.61 | 0.75 |
| 14 | 5.50 | 199.99 | 418.37 | 220.00 | 9706.89 | 0.75 |
| 15 | 6.32 | 200.00 | 420.00 | 220.00 | 8275.11 | 0.75 |
| 16 | 6.33 | 199.25 | 420.00 | 220.00 | 8213.65 | 0.74 |
| 17 | 6.41 | 199.98 | 420.00 | 220.00 | 8108.01 | 0.74 |
| 18 | 6.36 | 199.35 | 420.00 | 220.00 | 8167.57 | 0.74 |
| 19 | 6.36 | 198.51 | 420.00 | 220.00 | 8106.25 | 0.74 |
| 20 | 6.01 | 200.00 | 413.93 | 220.00 | 8699.79 | 0.74 |
| 21 | 6.44 | 199.94 | 417.20 | 220.00 | 7996.45 | 0.74 |
| 22 | 6.50 | 200.00 | 417.55 | 220.00 | 7893.72 | 0.73 |
| 23 | 6.46 | 200.00 | 416.18 | 220.00 | 7931.70 | 0.73 |
| 24 | 6.50 | 200.00 | 408.46 | 219.89 | 7702.87 | 0.71 |
| 25 | 5.50 | 177.57 | 420.00 | 220.00 | 8505.23 | 0.71 |
| 26 | 5.71 | 199.51 | 400.00 | 220.00 | 8931.96 | 0.70 |
| 27 | 6.50 | 200.00 | 403.81 | 219.52 | 7590.64 | 0.70 |
| 28 | 5.50 | 174.94 | 417.86 | 220.00 | 8325.26 | 0.70 |
| 29 | 6.50 | 200.00 | 402.11 | 219.62 | 7560.36 | 0.70 |

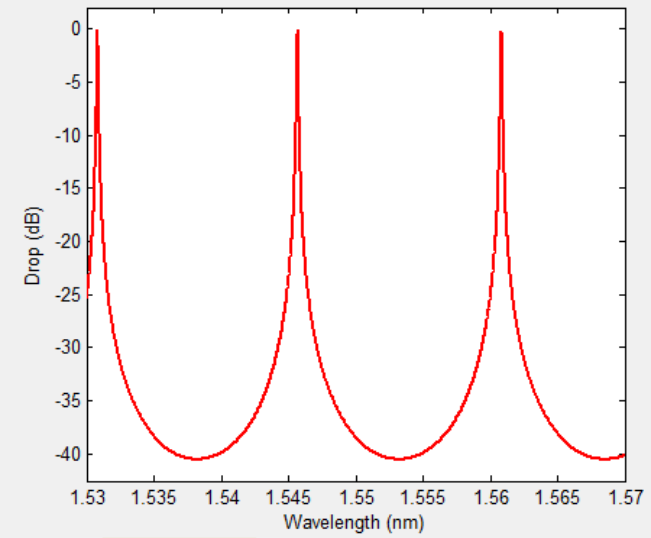


Figure 4: Drop port output channel response

The optimisation value was close to the confirmation test result with a percentage of error less than 5% and the details are listed in Table 6.

The optimum condition by the RSM is almost similar with the one obtained using mathematical modelling.

Table 6
Comparison of optimum condition between RSM-CCD and mathematical modelling

| Result | Q |
|---|---|
| RSM | 9192.79 |
| Confirmation test | 8739.81 |

## V. Conclusion

In designing a high-performance SOI microring channel dropping filter, effective parameters should be controlled and optimised. From the three-dimensional surface plots for the Q-factor optimisation, the ring radius is inversely

proportional to the Q-factor while the gap and core thickness is directly proportional to the Q-factor. Hence, large Q-factor can be obtained by increasing the gap and core thickness. It can also be concluded that waveguide width is insignificant and does not influence either in increasing or decreasing the Q-factor. The optimum condition generated by the RSM, which is based on the highest desirability and Q-factor value is when the ring radius is 5.50μm, a gap of almost 200nm, waveguide width of 418 nm and core thickness of 220 nm. As an extension to work carried out in this paper, the following future work may perform the RSM-CCD to evaluate the device parameter variations on other performance, such as Free Spectral Range (FSR) and finesse.

## ACKNOWLEDGEMENT

Our thanks to Universiti Teknikal Malaysia Melaka (UTeM) and Ministry of Higher Educations (MOHE) for the support. This research work is supported by funding from MOHE with the grant no: RACE/F3/TK2/FKEKK/F00298

## REFERENCES

[1] K. Padmaraju, K. Bergman, "Resolving the thermal challenges for silicon microring resonator devices," in *Nanophotonics*, vol. 3, issue 4-5, pp. 269–281, 2014.

[2] S. Song, X. Yi, S. X.Chew, L. Li, L. Nguyen, R. Zheng, "Optical single-sideband modulation based on silicon-on-insulator coupled-resonator optical waveguides," in *Optical Engineering*, vol. 55 (3), 031114 (Oct 20, 2015).

[3] A.R. Hanim, B. Mardiana, H. Hazura, S. Saari, "On the modulation phase efficiency of a silicon pin diode optical modulator," in *2010 IEEE International Conference on Photonics (ICP)Proc.*, Malaysia, 2010, pp. 1-3.

[4] H. Jayatilleka, K. Murray, M. Caverley, N. A. F. Jaeger, L. Chrostowski, and S. Shekhar "Crosstalk in SOI Microring Resonator-Based Filters," in *Journal of Lightwave Technology*, Vol. 34 (12), pp. 2886-2896, 2016.

[5] H. Hazura, S. Shaari, P.S. Menon, A.R.Hanim, B. Mardiana, "Application of statistical method to investigate the effects of design parameters on the performance of microring resonator channel dropping filter," in *Int. J. Numer. Model.*, 26, pp.670–679, 2013.

[6] Budi Mulyanti, P Susthitha Menon, Sahbudin Shaari, T Hariyadi, L Hasanah, Hazura Haroon, "Design and optimization of coupled Microring Resonators (MRRs) in silicon-on-insulator," in *Sains Malaysiana*, Vol. 32, No. 2, pp. 247-252, 2014.

[7] Hazura Haroon, Sahbudin Shaari, PS Menon, B Mardiana, AR Hanim, N Arsad, BY Majlis, WM Mukhtar, Huda Abdullah, "Design and characterization of multiple coupled microring based wavelength demultiplexer in silicon–on–insulator (SOI)," in *Journal of Nonlinear Optical Physics & Materials*, vol. 21, issue 01, pp. 1250004, 2012.

[8] G. K. Celep and K. Dincer, "Optimization of Parameters for Electrospinning of Polyacrylonitrile Nanofibers by the Taguchi Method," *International Polymer Processing*, Vol. 32, No. 4, pp. 508-514, 2017.

[9] H. Hazura, H. A. Razak., N.N.A Aziz, "Performance Enhancement Of Optical Microring Resonator Using Taguchi Method Experimental Design," in *ARPN Journal of Engineering and Applied Sciences*, 11(5), pp. 3212-3216, 2016.

[10] R. W. Emerson, "Design of Experiments. Optimization Methods: From Theory to Design," *In M. Cavazzuti*, pp. 13-41, 2016.

[11] P. K. Basu, B. M. *Semiconductor Laser Theory*, CRC Press, 2015.

[12] H. Hazura, S. Shaari, P.S. Menon, N. Arsad, A.R. Hanim, "Design Modeling and Characterizations os SOI-based Parallel Cascaded MRR Array (PCMMRA) By Coupled Mode Theory," in *Journal of Telecommunication, Electronic and Computer Engineering (JTEC)*, 7 (1), pp. 31-35, 2015.

[13] Z. Pheng, "Coupled Multiple Micro-Resonators Design And Active Semiconductor Micro-Resonator Fabrication", *Thesis Dissertation University Of Southern California*, 2007.

[14] H. Hazura, B. Mardiana, A. R. Hanim, P.S. Menon, N. Arsad, Z. F M, Napiah, "Impact of coupled resonator geometry on silicon-on insulator wavelength filter characteristics," in *2011 IEEE Regional Symposium on Micro and Nanoelectronics (RSM)*, Malaysia, 2011, pp. 380-382.

[15] S. Salehi , M. Noaparast, S. Z. Shafaei, "Response Surface Methodology (RSM) for Optimization of Chalcopyrite Concentrate Leaching With Silver-Coated Pyrite," in *Physicochem. Probl. Miner. Process*, 52(2), pp. 1023−1035, 2016.

[16] T. D. Sonani , D. Y. Kushwaha , G. D. Acharya, "Review Of Tool Wear Estimation Using Response Surface Methodology," in *International Journal of Advance Engineering and Research Development*, Vol. 3 (1), , pp. 147-150 2016.

[17] V. Alimirzaloo, V. Modanloo, "Minimization of the Sheet Thinning in Hydraulic Deep Drawing Process Using Response Surface Methodology and Finite Element Method," in *International Journal of Engineering*, Vol. 29 (2), pp. 264-273, 2016.

[18] M. Jourshabani, A. Badiei, N. Lashgari , G. M. Ziarani, "Application of Response Surface Methodology as an Efficient Approach for Optimization of Operational Variables in Benzene Hydroxylation to Phenol by V/SBA-16 Nanoporous Catalyst," in *J. Nanostruct.*, 6(2):, pp. 105-113, 2016.